AMERICAN ACADEMY OF OPHTHALMOLOGY®

Advanced Vision Analyzer–Virtual Reality Perimeter

Device Validation, Functional Correlation and Comparison with Humphrey Field Analyzer

Priya Narang, MS,[1] *Amar Agarwal, FRCS, FRCOphth,*[2] *Maheswari Srinivasan, MOptom, FIACLE,*[2] *Ashwin Agarwal, MS*[2]

Purpose: To evaluate the Advanced Vision Analyzer (AVA; Elisar Vision Technology) and to compare pointwise threshold sensitivity and functional correlation of Elisar Standard Algorithm (ESA) with the Swedish Interactive Threshold Algorithm (SITA) of the Humphrey Field Analyzer (HFA; Carl Zeiss Meditec, Inc).

Design: Prospective, cross-sectional, observational case series.

Participants: One hundred sixty eyes (85 control participants, 75 glaucoma patients) for functional assessment, 15 eyes for test–retest variability (TRV), 107 eyes for blind spot trial (45 normal eyes, 62 glaucoma eyes) were recruited consecutively. A separate group of participants was chosen for each assessment.

Methods: All participants underwent ESA and SITA Standard 24-2 testing, and 1 eye of each participant was selected randomly. Intraclass correlation coefficient (ICC), Bland-Altman, linear regression, mean bias (MB), and proportional bias analyses were quantified and assessed. Threshold measurements, TRV, and blind spot location accuracy were compared with those of the HFA.

Main Outcome Measures: Pointwise threshold sensitivity, sectoral mean sensitivity (MS), mean deviation (MD), pattern standard deviation (PSD), TRV, blind spot location, average test time were computed, and data were correlated.

Results: The mean time required to perform a field test with the AVA was 7.08 ± 1.55 minutes and with HFA was 6.26 ± 0.54 minutes ($P = 0.228$). The MS difference between AVA and HFA was −2.2 ± 2.3 dB in healthy participants ($P < 0.001$) and −2.6 ± 3.5 dB in participants with glaucoma ($P < 0.001$). The correlation coefficients for pointwise threshold values were moderately to strongly correlated for both the devices ($r = 0.68–0.89$). For MS, the overall ICC value was 0.893 ($P < 0.001$) with MB of 2.48 dB and a limits of agreement (LOA) of 10.90 (range, 7.93 to −2.97). For TRV, response variability decreased with an increase in sensitivity and increased with eccentricity. Blind spot location was accurate, and global indices of testing methods correlated well.

Conclusions: The AVA effectively captures threshold values for each point in the visual field. Adequate functional correlation suggests substantial equivalence between the AVA (ESA) and HFA (SITA Standard), implying that AVA may allow accurate assessment of visual field. *Ophthalmology Science 2021;1:100035* © *2021 by the American Academy of Ophthalmology. This is an open access article under the CC BY-NC-ND license (http://creativecommons.org/licenses/by-nc-nd/4.0/).*

Supplemental material available at www.ophthalmologyscience.org/.

Computerized automated perimetry is a standardized and an efficient method to evaluate a patient's visual field sensitivity. The Humphrey Field Analyzer (HFA; Carl Zeiss Meditec, Inc) incorporates the Swedish Interactive Threshold Algorithm (SITA) strategy,[1] and currently, the SITA Standard is the conventional threshold estimation procedure in most clinical settings.[1–3]

Head-mounted perimetry devices have been described[4–6] with the benefit of being especially useful in patients with physical disabilities. The authors report on the Advanced Vision Analyser (AVA; Elisar Vision Technology), a new portable, lightweight virtual reality headset perimeter with optics that allows visual field analysis to be performed under test conditions compatible with standard automated perimetry with eye-tracking and a cloud-based storage system that allows backup of data. The AVA incorporates a customized Elisar Standard Algorithm (ESA). This study aimed to describe and validate the device, evaluate pointwise threshold sensitivity, and substantiate the equivalence of ESA with the SITA Standard.

https://doi.org/10.1016/j.xops.2021.100035
ISSN 2666-9145/21

Methods

The study protocol conformed to the tenets of the Declaration of Helsinki, and institutional review board approval was sought from the local ethics committee at Dr. Agarwal's group of eye hospitals. All the participants gave informed consent before participation. The AVA was tested at Dr. Agarwal's Eye Institute and Research Centre (Chennai, India). All enrolled participants underwent a complete routine ophthalmologic examination, including best-corrected visual acuity measurement, applanation tonometry, slit-lamp biomicroscopy, optic disc stereoscopic photography, and posterior segment evaluation. The healthy participants formed the control group and were recruited from the outdoor patient department and were relatives of patients (except for patients with glaucoma) who volunteered to participate in the study. Inclusion criteria were: (1) a best-corrected visual acuity of 20/30 or better with an optimal refractive correction (< 5 diopters spherical equivalent), (2) intraocular pressure of less than 20 mmHg, (3) normal appearance of optic disc, (4) normal visual fields, and (5) pupil size of 3 mm or more for all test sessions.

Glaucoma was diagnosed by a glaucoma expert on the basis of the presence of glaucomatous optic neuropathy that was characterized by neuroretinal rim thinning, retinal nerve fiber layer defect, excavation, and cup-to-disc ratio asymmetry of 0.2 on optic disc stereophotographs and intraocular pressure of more than 22 mmHg. In addition, participants in the glaucoma group comprised individuals who were known to have glaucoma that was managed with topical medications and showed intraocular pressure of less than 21 mmHg. Eligible patients also were enrolled based on the data from a clinical registry of glaucoma clinics at our hospital. All patients with glaucoma had prior exposure to perimetry. The perimetry procedure was explained to all other participants in detail to minimize the learning curve effect and they underwent a trial test with both devices 1 day before the actual test. The results were discarded, and actual tests were performed again on the next day. Considering the patient's comfort, 1 eye with better visual acuity and lesser refractive error from each participant was chosen and tested. If both eyes showed similar visual acuity, 1 eye randomly was selected. Exclusion criteria were the presence of (1) cataract or any other ocular surgery (except uncomplicated cataract surgery), (2) neurologic disorder, (3) any systemic or ocular disease that could interfere with visual field results, and (4) amblyopia. Patients with false-positive, false-negative, and fixation loss results of more than 20% were excluded from the study.

Device

The AVA comprises 4 main components: a head-mounted device (HMD), a patient response (PR) button, a test controller device (TCD), and a backend cloud server.

Head-mounted device. The HMD (Fig 1) incorporates an optic and display subsystem that comprises a spectroscope with a liquid crystal display (LED). The screen is coupled with a convex lens system that presents a magnified virtual image at 60 cm, which is observed during test conditions. The optical system is dichoptic, and it separates the images presented to each eye, thereby obviating the need to occlude the other eye, although the test can also be performed binocularly. The monocular field of view achieved for each eye is 60 degrees (horizontal, vertical, and diagonal), which allows conducting the standard 30-2, 24-2, and 10-2 tests. The algorithms incorporated in the AVA include Full Threshold, Elisar Standard, and Elisar Fast. The AVA offers white-on-white perimetry with a single central fixation target after correction for lens distortion and field curvature. The lens holder has a provision for placing lenses to correct refractive error of the eyes being tested. The eye-tracking subsystem consists of 2 infrared complementary metal–oxide–semiconductor cameras placed for each eye and an array of infrared LEDs used to illuminate the pupil. The images of the pupil captured by the eye-tracking subsystem are transferred wirelessly to the TCD, where the operator can monitor the gaze of the patient for qualitative assessment. The frame rate of video on the TCD is 23 ± 2 frames per second.

Background illumination of the display is maintained at 9.6 cd/m^2, which can be controlled by changing the brightness and luminance of the screen. Goldman III size stimuli are presented for the range of 40 to 9 dB, whereas for achieving the range of 0 to 8 dB, stimulus size is increased at the intensity of 650 cd/m^2 as per Ricco and Piper spatial summation laws. Contrast levels from 9 to 40 dB are achieved by changing brightness of the stimulus, whereas for 0 to 8 dB, contrast is achieved by increasing the size according to the size-luminance equivalence. The stimuli projection time is 200 ms and the interstimulus interval varies from 1400 to 1800 ms, which is determined primarily by the PR rate. The test begins with a constant interstimulus interval of 1600 ms and adjusts to the PR rate after first 10 responses. The HMD has an adjustable headband and a knob to adjust for interpupillary distance.

To ensure a reliable result, catch trials are incorporated into the testing strategy that are conducted approximately once for every 10 stimuli presentations. False-positive catch trials are performed by looking for responses from patients when no stimuli are presented. False-negative catch trials are performed by presenting stimuli that are 3 dB more than a previously determined threshold sensitivity at a specific location in the visual field, the prerequisite being that the threshold sensitivity at that specific location is more than 11 dB. If a person does not respond to the brighter stimulus, it is considered a false-negative result.

Patient Response Button. The patient presses the PR button to record responses to the presented stimuli, and it communicates the time stamp at which the button is clicked. The information is recorded and used by the computing subsystem to determine the subsequent stimuli. If the response time is more than 1.5 seconds, the stimulus is deemed not seen.

Test Controller Device. The TCD is a tablet that is connected wirelessly to the HMD and to the cloud server. To set up a test, the administrator logs in and pairs it with the headset, followed by input of test details. The device adjusts for spherical error to a certain extent and displays appropriate trial lenses to be used for correction. The TCD can be used to interpret and analyze the results.

Backend Cloud Server. The cloud-based storage system allows users to obtain a backup of all the tests and reports and retrieve them when necessary.

Elisar Standard Algorithm

The ESA uses 2 prior curves that describe the probability distribution of threshold sensitivities of normals and abnormals. The prior probability curves of the threshold estimates are built using results recorded from a set of 100 participants. The detailed methods used to determine prior curves for normal and abnormal conditions is similar to the method explained by Turpin et al.[7]

The test starts at 4 seed locations based on the age-corrected normal mean value for that location. The 54 points are divided into 4 zones, and each of the zone has a seed point that is located 12.7° apart from fixation. The test eventually proceeds according to the HFA 24-2 growth pattern. Subsequent stimulus intensities are determined based on a 4-2-dB staircase procedure. The algorithm uses initial step sizes of 4 dB that are followed by 2 dB after the first reversal. While the staircase is running, the probability curves of threshold estimates are regenerated based on the response to the stimulus (seen or not seen). The new probability curves are determined by multiplying the old prior curves by a likelihood

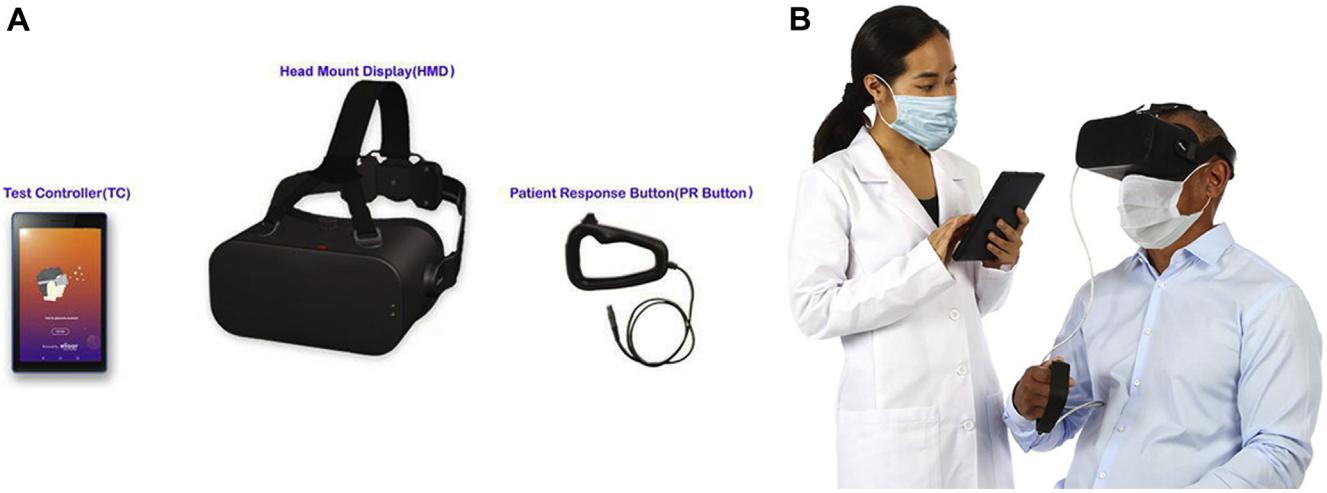

Figure 1. Images showing the Advanced Vision Analyzer (AVA). **A**, Components of the AVA: a head-mounted device (HMD), patient response (PR) button, and test controller. **B**, Patient and the instructor performing the visual field test with the AVA.

function that is similar in nature to the Zippy Estimation of Sequential Threshold (ZEST) algorithm.[8] They differ from the classic ZEST because the functions are scaled based on the threshold value and the 50% location is aligned to the stimulus intensity displayed. When the threshold value presented is less than the fifth percentile level of threshold estimates collected in the initial prior database, the likelihood function used for the abnormal probability curve has asymptotes of 20% and 80%, whereas the function used for the normal curve has asymptotes of 0% and 100%. The testing at a single location is terminated if (1) either of the probability curves of threshold estimates have a standard deviation that is less than a predetermined level (the level varies linearly from 2.5 dB for threshold estimates near 0 dB to 1.2 dB for threshold estimates near 40 dB) and (2) if 2 reversals of the staircase occur. The final threshold estimate is determined by considering the higher of the methods of final probability curves of thresholds. The primary difference between the ESA and ZEST algorithms is listed in Table 1.

Normative Database

Threshold measurements were performed on 174 eyes with 30-2 pattern, and the same database was used for the 24-2 test pattern. The age of participants ranged from 16 to 80 years (91 males and

Table 1. Primary Differences between the Elisar Standard and Zippy Estimation of Sequential Threshold Algorithms

Elisar Standard	Zippy Estimation of Sequential Threshold
Two separate prior curves (one assuming a normal subject and another assuming an abnormal subject) are used to determine posterior probabilities.	A single prior curve for determining posterior probabilities.
Posterior curves for both normal and abnormal conditions are estimated based on the responses to presented stimulus.	The posterior curve is estimated based on the responses to presented stimuli.
Next stimulus contrast level is determined based on the 4-2-dB staircase threshold method.	Next stimulus contrast level is the mean value of the posterior curve estimated based on response recorded by the patient.
End of test is defined as 1. Two reversals of the staircase or 2. Spread of the normal posterior curve is below a desired limit. The desired limit depends on the patient threshold value (higher for lower thresholds, lower for higher thresholds) or 3. Spread of the abnormal posterior curve is below a desired limit. The desired limit depends on the patient threshold value (higher for lower thresholds, lower for higher thresholds; 1 staircase quest)	End of test is defined as the point where the posterior curve standard deviation is less than a predefined limit. Example, 1.5 dB.
Final result is defined as the higher of modes of the normal or the abnormal posterior curves (1 staircase quest).	Final result is defined as the mean of the posterior curve.

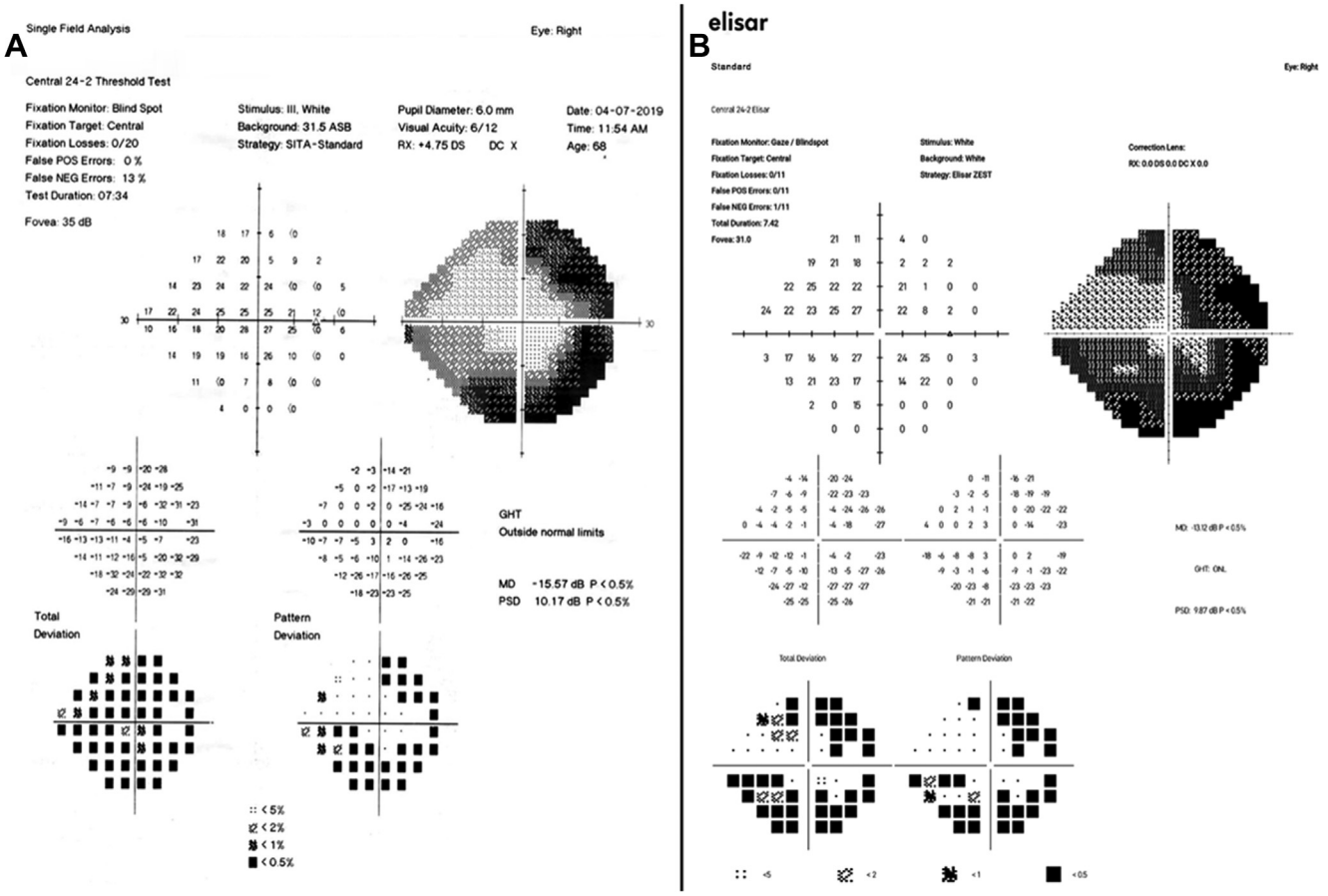

Figure 2. Printed test reports of the Humphrey Field Analyzer (HFA) Swedish Interactive Threshold Algorithm Standard and the Advanced Vision Analyzer (AVA). **A**, Clinical test report from the HFA of a patient with advanced glaucoma. **B**, Clinical test report from the AVA of the same patient (patient's name and registration number are masked).

83 females), and only 1 eye per participant was considered for the normative data. The database considered a linear model to account for participant age that was built after inverting all recorded threshold measurements to the right-eye orientation. The criteria for patient selection including inclusion and exclusion were same as mentioned for the control group. The other parameters that were captured from normative data collection study were (1) age-corrected means for all test points, (2) probability limits for absolute defects (total deviation) and localized defects (pattern deviation), and (3) probability limits for the mean deviation (MD) and pattern standard deviation (PSD). Participant ethnicity was not considered as a part of this database collection, and the data were collected from centers in Asia and Africa that comprised participants of mixed ethnic origin. To determine normal limits for each test location, a linear model was adopted, and regression was performed to calculate each point sensitivity value against age. All threshold estimates were converted to a 50-year-old equivalent based on the linear regression slope of sensitivity versus age, and probability limits were determined for this equivalent data. The method chosen to build normative data for AVA is similar to that reported by Heijl et al[9] and Anderson et al.[10]

Study Sample Size and Details. In all, 215 eyes were enrolled for the trial, and random execution of 24-2 ESA and SITA Standard was performed for the control and glaucoma group with an interval of 1 hour between the tests. After exclusion of participants with low reliability indices, 160 eyes (85 eyes in the control group and 75 eyes in the glaucoma group) were analyzed. Pointwise sensitivity was calculated for each point on the 24-2 grid along with the mean sensitivity (MS) value of all 52 points in the test, excluding 2 points around the blind spot,[11] and the values of both the devices were compared. As described by Asman and Heijl,[12] the visual field was divided into 10 sectors corresponding to normal retinal nerve fiber layer anatomic features, wherein the sectors in the inferior hemifield were mirror images of the sectors in the superior hemifield. Sectoral MS of each point in the sectors was calculated, and corresponding sectors of both the devices were compared. Sectoral MS analysis was performed to rule out any disparity in sectoral values. The MD and PSD were calculated and compared for both the devices.

Test–Retest Variability. The 24-2 strategy was repeated thrice on 15 eyes of 15 healthy volunteers. The tests were not performed more than twice on an individual participant on a single day. Based on eccentricity, the test locations were divided into 3 different zones: central (0°–10°), middle (10°–20°), and peripheral (20°–24°). The mean threshold values and standard deviations within each of the 3 zones were calculated for target locations. The proportion of test locations that differed more than 5 dB was spotted within each of the 3 visual field segments.

Blind Spot Location. The ability of AVA to localize the blind spot and detection of fixation loss by the Heijl Krakau blind spot

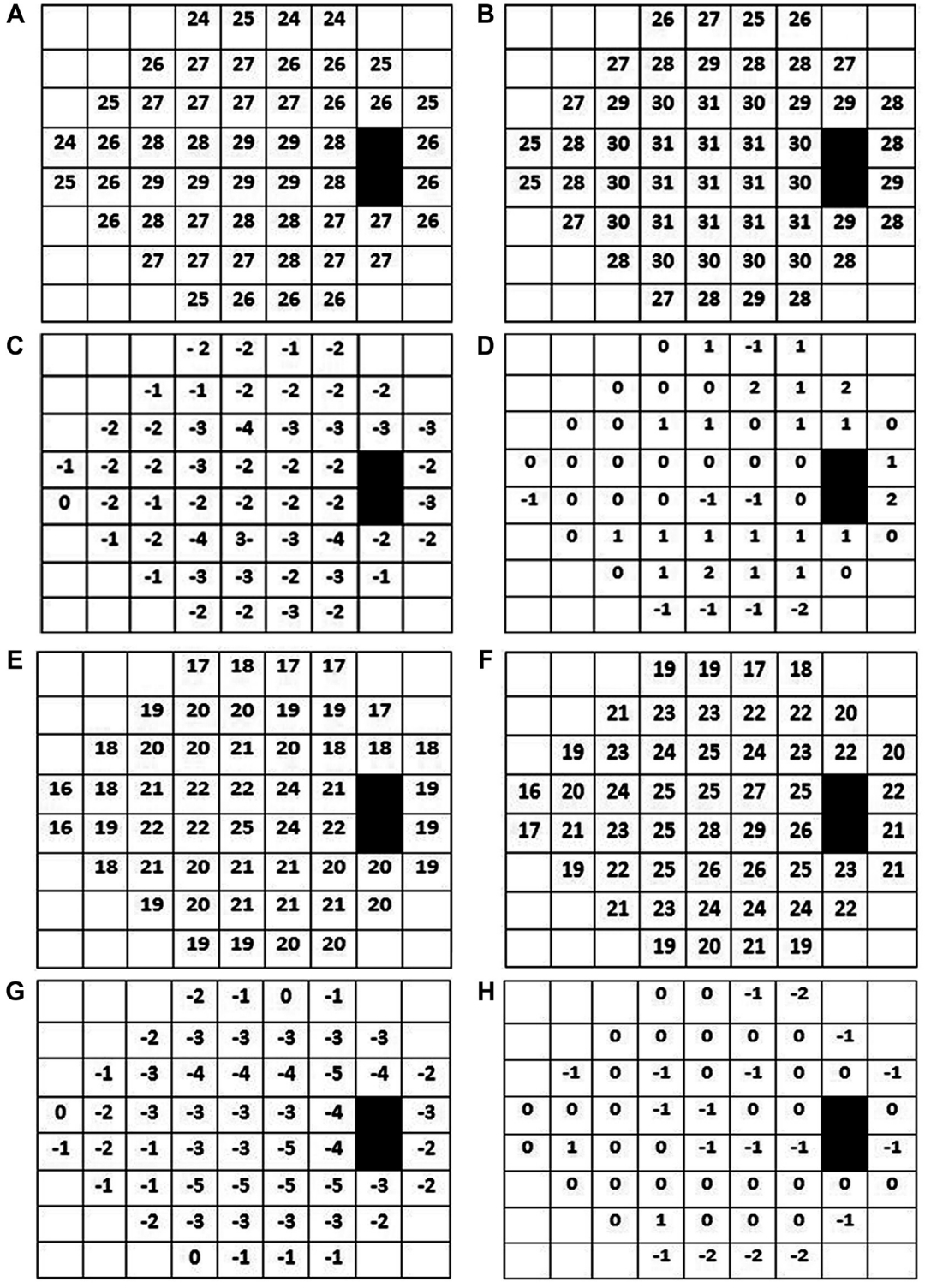

Figure 3. Pointwise sensitivity threshold values for the Advanced Vision Analyzer (AVA) and the Humphrey Field Analyzer (HFA) in healthy participants and patients with glaucoma. **A**, Mean sensitivity at each stimuli location for healthy participants with the AVA. **B**, Mean sensitivity at each stimuli location for healthy participants with the HFA (Swedish Interactive Threshold Algorithm [SITA] Standard). **C**, Difference in mean sensitivity at each stimuli location for healthy participants between the AVA and HFA. **D**, Difference in standard deviation at each stimuli location for healthy participants between the AVA and HFA. **E**, Mean sensitivity at each stimuli location for patients with glaucoma with the AVA. **F**, Mean sensitivity at each stimuli location for patients with glaucoma with the HFA (SITA Standard). **G**, Difference in mean sensitivity at each stimuli location for patients with glaucoma between the AVA and HFA. **H**, Difference in standard deviation at each stimuli location for patients with glaucoma between the AVA and HFA.

catch trial method[13,14] was performed in 45 eyes of healthy volunteers and 62 eyes of participants with glaucoma. The capability to maintain fixation by comparing the threshold measurements in the central 30° was performed and compared with the HFA. The threshold value along with fixation loss was noted and recorded for both the devices.

Statistical Analysis

IBM SPSS Statistics version 21.0 was used to calculate the intraclass correlation coefficient (ICC) to analyze the degree of correlation. Microsoft Excel (Microsoft) was used to plot a Bland-Altman graph that analyzed and quantified the limits of agreement (LOA) between the 2 devices. Ninety-five percent confidence intervals were calculated, and a P value of less than 0.05 was considered statistically significant. The presence of proportional bias for a variable was calculated by regressing the difference between the variable and the mean variable for both devices. The significance value (P value) of the linear regression model was applied to detect the presence of proportional bias, and it was considered to be significant for P values of less than 0.05. Test duration for each test was noted, and the values were compared using the Mann−Whitney U test. Data normality was evaluated using the Shapiro−Wilk test. Pearson's correlation coefficient (r) was applied to compare the corresponding parameters of both devices. Linear regression analysis was adopted to understand the relationship between 2 variables. The Wilcoxon signed-rank test was performed to compare the threshold values in the expected blind spot area for both control participants and glaucoma patients.

Results

The mean age of normal participants enrolled in the study was 38.21 ± 15.59 years and for the participants with glaucoma group was 56.72 ± 13.15 years. The mean time required to perform the visual field test with the AVA and HFA was 7.08 ± 1.55 minutes and 6.26 ± 0.54 minutes ($P = 0.228$, Mann−Whitney U test), respectively. No significant difference for the mean test time was detected when the healthy and glaucoma groups were compared. The full aperture trial lenses did not cause any lens rim artifact. The printed test reports of participants who underwent visual field testing with the HFA and AVA are presented in Figure 2.

Pointwise Sensitivity

The MS for healthy participants was 26.63 ± 2.36 dB for the AVA and 28.80 ± 2.16 dB for the HFA, and the difference between both the device was −2.2 ± 2.3 dB ($P < 0.0001$). The MS for patients with glaucoma was 19.75 ± 7.72 dB for the AVA and 22.34 ± 7.96 dB for the HFA, and the difference between both was −2.6 ± 3.5 dB ($P < 0.001$). Pointwise mean retinal sensitivity values obtained with both devices from healthy and glaucoma participants along with the pointwise difference in sensitivity and standard deviation at each stimuli location are presented in Figure 3. The Pearson's correlation coefficient was calculated for each point on the visual field that ranged from 0.68 to 0.89 ($P < 0.001$; Fig 4). When the point sensitivities were examined, an overall decrease in values with the AVA was noted, with no specific pattern observed in any visual field sector. The sensitivity values when divided into quartiles depicted a variation that was present throughout the entire range of sensitivities. The LOA (Bland-Altman analysis) were narrow for a higher range of sensitivity as compared with lower sensitivity.

Sectoral Sensitivity

Supplemental Table 1 denotes the overall and sectoral MS values and Supplemental Table 2 denotes the ICC values, mean bias (MB), proportional bias, and 95% LOA values. The Bland-Altman plot denoted 95% of data within the LOA (Fig 5A), and the linear regression analysis plot denoted good reliability (Fig 5B). The ICC value for the control group was 0.495 and for glaucoma group was 0.902, whereas the overall ICC value was 0.893. The correlation values were statistically significant for MS and sectoral MS, with $P < 0.001$ indicating a significant correlation in all cases.

Mean Deviation and Pattern Standard Deviation

For MD, ICC was 0.883 ($P < 0.001$), with MB of −0.23 dB (Supplemental Table 3) and LOA of 11.71 (range, 5.62 to −6.09). For PSD, the ICC was 0.751 ($P < 0.001$) with a MB of −0.21 dB (Supplemental Table 4) and LOA of 6.46 (range, 3.02 to −3.44). Supplemental Figure 1 depicts the Bland-Altman plot and linear regression analysis for MD and PSD. Proportional bias was present for PSD in the overall analysis as well as for glaucomatous patients.

Assessment of Test−Retest Variability

Linear regression analysis demonstrated an increase in eccentricity from one zone to the other with a simultaneous and corresponding increase in variability by 0.35 dB ($P < 0.001$). Supplemental Figure 2A depicts an increase in variability with an increase in eccentricity (slope, 0.35; intercept, 0.09). Linear regression analysis to plot the relationship between sensitivity and response variability depicted an increase in sensitivity with a relative decrease in response variability (Supplemental Fig 2B). The regression analysis portrayed that the relationship among false-positive findings ($P = 0.493$), false-negative findings ($P = 0.703$), fixation loss findings ($P = 0.755$), and the response variability were not statistically significant.

Assessment of Blind Spot

The mean threshold values at the presumed blind spot with the HFA and AVA in control participants and glaucoma patients are shown in Supplemental Table 5 ($P > 0.1$). The mean of fixation loss in percentage for the HFA and AVA demonstrated no statistically significant difference between groups, denoting the fixation accuracy of the AVA to be comparable with that of the HFA.

Discussion

The ZEST algorithm has been reported to be computationally simple as compared with the SITA, with test times being more consistent regardless of visual field defects.[7,15]

			0.75	0.78	0.70	0.76		
		0.76	0.73	0.76	0.77	0.78	0.80	
	0.79	0.77	0.80	0.83	0.80	0.80	0.78	0.74
0.73	0.80	0.82	0.84	0.86	0.77	0.75		0.73
0.69	0.70	0.88	0.84	0.74	0.59	0.75		0.77
	0.85	0.89	0.82	0.79	0.78	0.76	0.77	0.84
		0.79	0.87	0.78	0.77	0.74	0.83	
			0.70	0.68	0.73	0.71		

Figure 4. Correlation coefficient (*r*) between testing methods for pointwise threshold values (for all participants).

The key difference in the ESA was the use of a separate prior curve describing a glaucomatous population that allows the ESA to terminate more quickly in patients with glaucoma. Another difference that allows the ESA to account for an increase in variability at lower threshold levels is achieved by setting the termination limit dependent on the threshold value being tested.

While maximizing the operating range on a portable perimeter, the highest value of 9.6 cd/m^2 was adopted. The screen was calibrated by using a luminance measurement scheme, and calibration was verified by checking the contrast levels achieved, the limits for which were in agreement with International Organization for Standardization standard 12866 for ophthalmic perimeters.

For test–retest variability, the AVA demonstrated similar results to the HFA wherein on transition from a central to peripheral visual field segment, lowest proportion of locations displayed differences of more than 5 dB on repeat tests.[16] Peer studies report an increase in variability in the visual field from the central 10° to 30° in periphery[16,17] and also postulated that variability increases with a decrease in sensitivity.[18–21] Our analysis depicted similar results and are in agreement with previous studies.[22,23] Blind spot location accuracy of the AVA was comparable with that of the HFA, and no lens–rim artifact was detected.

For pointwise sensitivity analysis, the AVA demonstrated lower threshold values as compared with the HFA, which can be attributed to the difference in the thresholding algorithm. Alternatively, peer studies have documented that the SITA Standard program inherently tends to estimate higher values on pointwise sensitivity analyses when compared with the full-threshold strategy.[24,25] The correlation coefficient (*r*) for the pointwise threshold was correlated moderately to strongly for both the devices. The standard deviation in the glaucoma group, although comparable, was higher for both the devices. This could be ascribed to the higher variation and unequal distribution of patients with a varied degree of glaucoma severity.

The overall population and glaucoma group depicted ICC values for MS and sectoral MS analysis of more than 0.781 (range, 0.781–0.902) for the entire visual field, whereas it was observed to be less for the control group (range, 0.025–0.495). Apart from MS, the correlation coefficient of the MD and PSD also was observed to be less for the control group. The correlation values depend on the range of measurement; the wider ranges being assessed (as in glaucoma) often result in higher correlations than the narrower ranges (as in control participants).[26] The ICC values were statistically significant ($P < 0.001$), indicating a significant correlation in all cases. In Bland-Altman

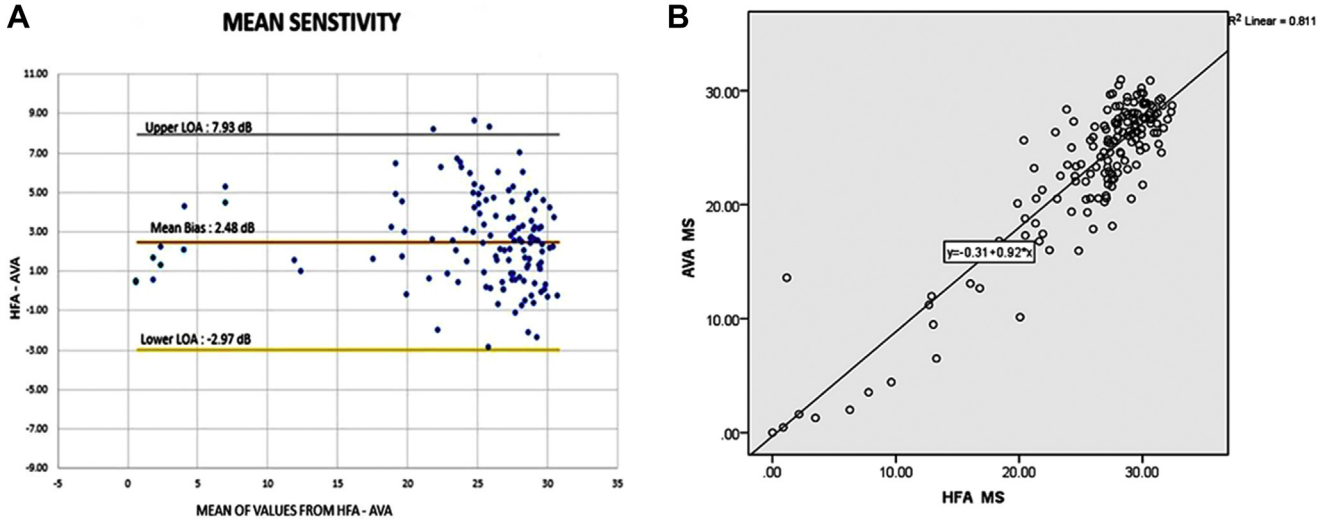

Figure 5. Bland-Altman plot and linear regression analysis of mean sensitivity (MS) values of the Humphrey Field Analyzer (HFA) and the Advanced Vision Analyzer (AVA). **A**, Bland-Altman plot for MS values between the HFA and AVA with upper limit of agreement (LOA) being 7.93 and lower LOA being −2.97 dB, with a mean bias of 2.48 dB. **B**, Linear regression analysis with the slope of 0.31 and an intercept of 0.92 with $R^2 = 0.811$. The plot indicates good reliability between mean sensitivity values of the HFA and AVA.

plots, the differences between both the devices were plotted using bar graphs to check for normality, and the differences were distributed normally, with 95% of data points lying within the upper and lower LOA. The difference in PSD values, when plotted against the mean of MS values, demonstrated a linear relationship ($P < 0.001$). The variation observed can be attributed not only to the difference in the type of device, but also to the expected variation that is encountered when the test is repeated with the same device. Additionally, an expected proportional bias in MS values obtained from the study population was found that adds to the aspect of variability. Proportional bias was present in few sectors for MS and PSD values that can be ascribed to the increased range of measurements observed in patients with advanced glaucoma. Studies have demonstrated that when sensitivity values decrease beyond 15 to 19 dB, the global indices and visual field index are affected, and the reports should be interpreted with caution as the values become unreliable.[27,28] Hence, after exclusion of data with threshold values of less than 19 dB and on reanalysis, no proportional bias was detected in any of the patients for MS and PSD. The range of MB values in the literature that describes interdevice variation in perimetry devices[29–31] were observed to be ±3 dB for MS, ±2 dB for MD, and ±1.5 dB for PSD. The values derived in our studies lie within the prescribed limits suggestive of AVA having a potential to serve as a diagnostic tool for visual field imaging.

Scope and Limitations

The AVA is a portable device weighing 500 g, and it can play a pivotal role in performing perimetry in bedridden patients with neck or spine deformities. The AVA also can be used for performing visual field tests in rural areas of developing countries where patients do not have direct access to tertiary care hospitals. During the coronavirus disease 2019 pandemic and in the era afterward, the AVA allows performing the test with adequate physical distance, and patient can perform the test while wearing a facemask (Fig 1B). The limitations are that the AVA does not have an active eye-tracking system, and it may be unreliable in individuals with abnormal and eccentric pupils. Second, for achieving the range of 0 to 8 decibels, the stimulus size is increased, and it is assumed that Ricco's law pertains in this situation, although this was not tested. The MS difference levels observed with the AVA could be related to either the algorithm and novelty of the test setup or to aspects that need further evaluation. Additionally, the diagnostic precision of the AVA needs to be assessed and currently is beyond the scope of this article.

In summary, considering the significance levels of ICC values, Bland-Altman plots, linear regression analysis, pointwise sensitivity correlation, and absence of proportional bias, the authors contemplate that the results demonstrate functional equivalence between the AVA and the HFA. However, further studies with larger numbers of patients and detailed clinical evaluation for the actual diagnostic accuracy of the AVA are required to allow for definite conclusions.

Acknowledgments

The authors thank Vamsi Chintalapati, BTech, MTech, Indian Institute of Technology, Chennai, India, developer of the device, for his help and tremendous efforts continuously to improvise the device during various stages of the study and Rhea Narang for providing technical assistance.

Footnotes and Disclosures

Originally received: January 2, 2021.
Final revision: June 4, 2021.
Accepted: June 21, 2021.
Available online: June 25, 2021. Manuscript no. D-21-00002.

[1] Refractive & Glaucoma Services, Narang Eye Care & Laser Centre, Ahmedabad, India.

[2] Dr. Agarwal's Eye Hospital & Research Centre, Chennai, India.

Presented in part as a poster at: American Academy of Ophthalmology Annual Meeting, October 27-30, 2018, Chicago, Illinois.

Disclosure(s):
All authors have completed and submitted the ICMJE disclosures form.

The author(s) have no proprietary or commercial interest in any materials discussed in this article.

The Advanced Vision Analyzer is authorized for sale and distribution in the United States by the United States Food and Drug Administration. Dr. Amar Agarwal has an indirect financial interest in the product, but it does not have any potential competing interest in this study. No patents are pending for the device Advanced Vision Analyzer.

HUMAN SUBJECTS: Human subjects were included in this study. The study protocol conformed to the Declaration of Helsinki and Institutional Review Board approval was sought from the local ethics committee. All subjects gave informed consent prior to participation.

No animal subjects were included in this study.

Author Contributions:

Conception and design: Narang

Analysis and interpretation: Narang, Agarwal, Srinivasan, Agarwal

Data collection: Narang, Agarwal, Srinivasan, Agarwal

Obtained funding: N/A

Overall responsibility: Narang, Agarwal

Abbreviations and Acronyms:
ESA = Elisar Standard Algorithm; **HMD** = head-mounted device; **ICC** = intraclass correlation coefficient; **LOA** = limits of agreement; **MB** = mean bias; **MD** = mean deviation; **MS** = mean sensitivity; **PR** = patient response; **PSD** = pattern standard deviation; **SITA** = Swedish Interactive Threshold Algorithm; **ZEST** = Zippy Estimation of Sequential Threshold.

Keywords:
Advanced vision analyzer, AVA, Elisar, Elisar Standard, HFA, Humphrey Field Analyzer, Perimetry, SITA Standard, Virtual reality perimeter, Visual field, ZEST.

Correspondence:
Priya Narang, MS, Narang Eye Care & Laser Centre, Aeon Complex, Second Floor, Vijay Cross Roads, Ahmedabad 380009, India. E-mail: narangpriya19@gmail.com.

References

1. Bengtsson B, Heijl A, Olsson J. Evaluation of a new threshold visual field strategy, SITA, in normal subjects. Swedish Interactive Threshold Algorithm. *Acta Ophthalmol Scand*. 1998;76(2):165−169.
2. Bengtsson B, Heijl A. Evaluation of a new perimetric threshold strategy, SITA, in patients with manifest and suspect glaucoma. *Acta Ophthalmol Scand*. 1998;76(3):268−272.
3. Budenz DL, Rhee P, Feuer WJ, et al. Sensitivity and specificity of the Swedish Interactive Threshold Algorithm for glaucomatous visual field defects. *Ophthalmology*. 2002;109(6):1052−1058.
4. Hollander DA, Volpe NJ, Moster ML, et al. Use of a portable head mounted perimetry system to assess bedside visual fields. *Br J Ophthalmol*. 2000;84(10):1185−1190.
5. Wroblewski D, Francis BA, Sadun A, et al. Testing of visual field with virtual reality goggles in manual and visual grasp modes. *Biomed Res Int*. 2014;2014:206082.
6. Matsumoto C, Yamao S, Nomoto H, et al. Visual field testing with head-mounted perimeter 'imo.'. *PLoS One*. 2016;11(8):e0161974.
7. Turpin A, McKendrick AM, Johnson CA, Vingrys AJ. Properties of perimetric threshold estimates from full threshold, ZEST, and SITA-like strategies, as determined by computer simulation. *Invest Ophthalmol Vis Sci*. 2003;44(11):4787−4795.
8. King-Smith PE, Grigsby SS, Vingrys AJ, et al. Efficient and unbiased modifications of the QUEST threshold method: theory, simulations, experimental evaluation and practical implementation. *Vision Res*. 1994;34(7):885−912.
9. Heijl A, Lindgren G, Olsson J. Normal variability sof static perimetric threshold values across the central visual field. *Arch Ophthalmol*. 1987;105:1544−1549.
10. Anderson AJ, Johnson CA, Fingeret M, et al. Characteristics of the normative database for the Humphrey matrix perimeter. *Invest Ophthalmol Vis Sci*. 2005;46(4):1540−1548.
11. Bengtsson B, Olsson J, Heijl A, Rootzén H. A new generation of algorithms for computerized threshold perimetry, SITA. *Acta Ophthalmol Scand*. 1997;75(4):368−375.
12. Åsman P, Heijl A. Glaucoma hemifield test: automated visual field evaluation. *Arch Ophthalmol*. 1992;110(6):812−819.
13. Safran AB, Mermoud C, Mermillod B. A strategy for measuring the blind spot using automated perimetry. *Neuro-ophthalmology*. 1993;13(6):303−308.
14. Asman P, Fingeret M, Robin A, et al. Kinetic and static fixation methods in automated threshold perimetry. *J Glaucoma*. 1999;8(5):290−296.
15. Vingrys AJ, Pianta MJ. A new look at threshold estimation algorithms for automated static perimetry. *Optom Vis Sci*. 1999;76(8):588−595.
16. Lewis RA, Johnson CA, Keltner JL, Labermeier PK. Variability of quantitative automated perimetry in normal observers. *Ophthalmology*. 1986;93(7):878−881.
17. Greve EL. Single and multiple stimulus static perimetry in glaucoma; the two phases of perimetry. *Doc Ophthalmol*. 1973;36:1−353.
18. Holmin C, Krakau CET. Variability of glaucomatous visual field defects in computerised perimetry. *Graefes Arch Exp Ophthalmol*. 1979;210(4):235−250.
19. Wilensky JT, Joondeph BC. Variation in visual field measurements with an automated perimeter. *Am J Ophthalmol*. 1984;97(3):328−331.
20. Katz J, Sommer A. Asymmetry and variation in the normal hill of vision. *Arch Ophthalmol*. 1986;104(1):65−68.
21. Parrish II RK, Schiffman J, Anderson DR. Static and kinetic visual field testing; reproducibility in normal volunteers. *Arch Ophthalmol*. 1984;102(10):1497−1502.
22. Weber J, Rau S. The properties of perimetric thresholds in normal and glaucomatous eyes. *German J Ophthalmol*. 1992;1(2):79−85.
23. Chauhan B, Tompkins J, LeBlanc R, McCormick T. Characteristics of frequency-of-seeing curves in glaucoma in normal subjects, patients with suspected glaucoma, and patients with glaucoma. *Invest Ophthalmol Vis Sci*. 1993;34(13):3534−3541.
24. Bengtsson B, Heijl A. SITA Fast, a new rapid perimetric threshold test: description of methods and evaluation in patients with manifest and suspect glaucoma. *Acta Ophthalmol Scand*. 1998;76:431−437.
25. Artes PH, Iwase A, Ohno Y, et al. Properties of perimetric threshold estimates from Full Threshold, SITA Standard, and SITA Fast strategies. *Invest Ophthalmol Vis Sci*. 2002;43(8):2654−2659.
26. Bunce C. Correlation, agreement, and Bland−Altman analysis: statistical analysis of method comparison studies. *Am J Ophthalmol*. 2009;148(1):4−6.
27. Gardiner SK, Swanson WH, Goren D, et al. Assessment of the reliability of standard automated perimetry in regions of glaucomatous damage. *Ophthalmology*. 2014;121(7):1359−1369.
28. Blumenthal EZ, Sample PA, Berry CC, et al. Evaluating several sources of variability for standard and SWAP visual fields in glaucoma patients, suspects, and normals. *Ophthalmology*. 2003;110(10):1895−1902.
29. Rowe FJ, Wishart M, Spencer S. Perimetry comparisons for Octopus G Top and dynamic programmes versus Humphrey 24−2 SITA Fast and SITA Standard programmes. *Ophthalmol Res*. 2014;2(1):24−42.
30. Kimura T, Matsumoto C, Nomoto H. Comparison of head-mounted perimeter (imo) and Humphrey Field Analyzer. *Clin Ophthalmol*. 2019;13:501−513.
31. Kong YXG, He M, Crowston JG, Vingrys AJ. A comparison of perimetric results from a tablet perimeter and Humphrey Field Analyzer in glaucoma patients. *Transl Vis Sci Technol*. 2016;5(6):2.